

2006

## Phylogenetics of the "Tiger-flower" Group (Tigridieae: Iridaceae): Molecular and Morphological Evidence

Aaron Rodriguez

*University of Wisconsin-Madison; Universidad de Guadalajara*

Kenneth J. Sytsma

*University of Wisconsin-Madison*

Follow this and additional works at: <http://scholarship.claremont.edu/aliso>



Part of the [Botany Commons](#)

---

### Recommended Citation

Rodriguez, Aaron and Sytsma, Kenneth J. (2006) "Phylogenetics of the "Tiger-flower" Group (Tigridieae: Iridaceae): Molecular and Morphological Evidence," *Aliso: A Journal of Systematic and Evolutionary Botany*: Vol. 22: Iss. 1, Article 33.

Available at: <http://scholarship.claremont.edu/aliso/vol22/iss1/33>

PHYLOGENETICS OF THE “TIGER-FLOWER” GROUP (TIGRIDIEAE: IRIDACEAE):  
MOLECULAR AND MORPHOLOGICAL EVIDENCE

AARON RODRIGUEZ<sup>1,3</sup> AND KENNETH J. SYTSMA<sup>1,2</sup>

<sup>1</sup>Department of Botany, University of Wisconsin, 430 Lincoln Dr., Madison, Wisconsin 53706, USA

<sup>2</sup>Corresponding author (kjsytsma@wisc.edu)

ABSTRACT

The phylogenetic relationships among 23 species of the tribe Tigridieae (Iridaceae) were inferred using morphological data and nucleotide sequences from nuclear ITS and three intergenic spacers of the cpDNA: *psbA-trnH*, *trnT-trnL*, and *trnL-trnF*. Although all data sets supported a monophyletic Mexican-Guatemalan Tigridiinae including two taxa usually placed in Cipurinae (*Cardiostigma longispatha* and *Nemastylis convoluta*), neither morphology, cpDNA, nor ITS resolved phylogenetic relationships within this lineage. A graphical tree of trees analysis showed the cladograms derived from morphology to be the most topologically distinct within the set of all trees examined and to be the set with most divergent trees. Finally, cladistic analysis of the combined data sets supported the recurrent dispersal of Cipurinae from South to North America and a South American origin of the Mexican-Guatemalan subtribe Tigridiinae.

Key words: Cipurinae, cpDNA, internal transcribed spacer (ITS), Iridaceae, phylogenetics, *psbA-trnH*, Tigridieae, Tigridiinae, *trnL-trnF*, *trnT-trnL*.

INTRODUCTION

The Iris family, Iridaceae, is a group of perennial herbs that includes horticulturally important genera such as *Crocus* L., *Freesia* Eckl. ex Klatt, *Gladiolus* L., and *Iris* L. The family is distributed worldwide in both tropical and temperate regions, but South Africa, the eastern Mediterranean, Mexico, and South America are especially species-rich. Iridaceae are distinguished by having leaves with a bifacial, equitant, sheathing base and a unifacial (isobilateral) blade, flowers with three stamens, and, with the exception of monotypic *Isophysis*, an inferior ovary. The morphological distinctiveness of Iridaceae has generated little controversy over its status and circumscription except for the treatment of *Isophysis tasmanica* (Hook.) T. Moore (Tasmania) and the saprophytic *Geosiris aphylla* Baill. (Madagascar), both of which have been treated as separate families (Dahlgren et al. 1985; Goldblatt 1990; Rudall 1994; Chase et al. 1996). Molecular studies based on cpDNA sequences showed Iridaceae to be a monophyletic group with the genus *Isophysis* as sister to all other members of the family (Souza-Chies et al. 1997; Reeves et al. 2001). Goldblatt (1990) subdivided Iridaceae into the subfamilies Isophysidoideae, Nivenioideae, Ixoideae, and Iridoideae. He further divided subfamily Iridoideae into the tribes Iridae, Mariceae, Sisyrinchieae, and Tigridieae.

The tribe Tigridieae is strictly a New World group with centers of diversity in temperate and Andean South America and Mexico. The tribe comprises plants with curiously formed and highly colored flowers that exhibit great morphological variation, making many species potentially valuable as cultivated plants. The style branches frequently form a specialized and complex structure intimately associated

with the stamens, with the latter also quite specialized. Such elaborate floral structures contrast with the vegetative uniformity in the tribe. All species develop underground bulbs and possess plicated or foliated leaves. Tigridieae have been subdivided into the subtribes Tigridiinae and Cipurinae (Goldblatt 1990). A gametophytic chromosome number of  $n = 14$  and disulcate pollen grains characterize subtribe Tigridiinae. The group is centered in Mexico and Guatemala, but eight species of *Tigridia* occur natively in Peru and Chile. Conversely, subtribe Cipurinae possess monosulcate pollen grains and a gametophytic chromosome number of  $n = 7$ . Cipurinae have a center of diversification in South America, with some species extending north into the southern USA. The bimodal geographical distribution of Tigridieae raises interesting questions concerning the phylogenetic and biogeographic relationships of the taxa in the two regions.

The tribe Tigridieae is taxonomically difficult and phylogenetically poorly understood. Thus, cladistic analysis of both morphology and molecules is needed. The flowers display great variation in color, shape, and structure, but unfortunately the flowers are very ephemeral and preserve poorly as herbarium specimens. Both the extensive floral variation and poor flower preservation have led to a confusing taxonomy of the group and the establishment of 40 distinct genera, several of them monotypic. Generic boundaries, species affiliations, and phylogenetic relationships are problematic and vary considerably from one specialist to another. In the latest morphology-based phylogenetic treatment of the Tigridieae (Goldblatt 1990), only 18 genera are recognized. The genera *Alophia* Herb., *Cobana* Ravenna, *Fosteria* Molseed, *Sessilanthera* Molseed & Cruden, and *Tigridia* Juss. are placed in Tigridiinae, whereas *Ainea* Ravenna, *Calydorea* Herb., *Cardenanthus* R. C. Foster, *Cipura* Aubl., *Cypella* Herb., *Eleutherine* Herb., *Ennealophus* N. E. Br., *Gelasine* Herb., *Herbertia* Sweet, *Kelissa* Ravenna, *Mastigostyla* I. M.

<sup>3</sup> Present address: Departamento de Botánica y Zoología, Universidad de Guadalajara, Apartado Postal 139, 45101 Zapopan, Jalisco, Mexico (rca08742@cucba.udg.mx)

Table 1. Taxa and accessions examined for morphological, nrDNA, and cpDNA variation. Taxa are alphabetically arranged.

Taxon	Voucher	Locality
<i>Alophia veracruzana</i> Goldblatt & Howard	Yucca Do Nursery	Mexico. Veracruz
<i>Calydorea pallens</i> Griseb.	San Antonio Botanical Gardens	Unknown
<i>Cardiostigma longispatha</i> (Herb.) Baker	Rodriguez 2794	Mexico. Mexico: Tejupilco de Hidalgo
<i>C. longispatha</i> (Herb.) Baker	Rodriguez 2798	Mexico. Mexico: Tejupilco de Hidalgo
<i>Cipura campanulata</i> Ravenna	Rodriguez 2893	Mexico. Guerrero: Mochitlin
<i>C. campanulata</i> Ravenna	Rodriguez & Suarez 2710	Mexico. Nayarit: San Pedro Lagunillas
<i>Cobana guatemalensis</i> (Standl.) Ravenna	Rodriguez et al. 2831	Guatemala. Alta Verapaz: Pueblo Viejo
<i>Cypella rosei</i> R. C. Foster	Rodriguez & Martinelli 2855	Mexico. Nayarit: Compostela
<i>Eleutherine latifolia</i> (Standl. & L. O. Williams) Ravenna	Rodriguez 2722	Mexico. San Luis Potosi: Rayon
<i>Ennealophus foliosus</i> (Kunth) Ravenna	Castillo 2001	Ecuador. Pichincha: Pulumahua
<i>Fosteria oaxacana</i> Molseed	Rodriguez & Villegas 2754	Mexico. Oaxaca: Nochixtlan
<i>Iris versicolor</i> L.	Rodriguez s. n.	USA. Wisconsin: Ashland
<i>Nemastylis convoluta</i> Ravenna	Ramirez 3390	Mexico. Jalisco: El Tuito
<i>N. tenuis</i> (Herb.) Baker	Rodriguez 2636	Mexico. Jalisco: San Miguel el Alto
	Rodriguez & Villand 2648	Mexico. Jalisco: Guadalajara
	Southwestern Native Seeds, Tucson	USA. Arizona: Cochise
<i>Neomarica gracilis</i> (Herb.) Sprague	Rodriguez s. n.	Unknown. Greenhouse, University of Wisconsin, Madison
<i>Rigidella flammea</i> Lindl.	Rodriguez et al. 2813	Mexico. Michoacan: Cd. Hidalgo
<i>R. immaculata</i> Herb.	Rodriguez et al. 2832	Guatemala. Sacatepequez: Antigua
<i>R. inusitata</i> Cruden	Rodriguez 2890	Mexico. Guerrero: Chichihualco
<i>R. orthantha</i> Lem.	Rodriguez & Villegas 2739	Mexico. Oaxaca: Evangelista
<i>Sessilanthera citrina</i> Cruden	Rodriguez 2892	Mexico. Guerrero: Chichihualco
<i>S. heliantha</i> (Ravenna) Cruden	Rodriguez 2885	Mexico. Guerrero: Chichihualco
<i>S. latifolia</i> (Weath.) Molseed & Cruden	Rodriguez & Vargas 2791	Mexico. Guerrero: Iguala
<i>Sisyrinchium scabrum</i> Schldl. & Cham.	Rodriguez 2621	Mexico. Jalisco: Tapalpa
<i>Tigridia durangense</i> Molseed	Rodriguez and Vargas 2642	Mexico. Durango: El Salto
<i>T. huajuapense</i> Molseed ex Cruden	Rodriguez & Villegas 2738	Mexico. Oaxaca: Huajuapán de León
<i>T. lutea</i> Link, Klotzsch & Otto	Calcinos s. n.	Peru. Lima: Lomas de Lurin
<i>T. mexicana</i> Molseed subsp. <i>mexicana</i>	Rodriguez 2805	Mexico. Mexico: Valle de Bravo
<i>T. multiflora</i> (Baker) Ravenna	Rodriguez 2625	Mexico. Jalisco: Tapalpa
<i>Trimezia fosteriana</i> Steyerem.	Rodriguez & Suarez s. n.	Unknown. Mexico. Jalisco: Guadalajara; cultivated
<i>T. martinicensis</i> Herb.	Hahn 7656	French West Indies. Guadeloupe Island

Johnst., *Nemastylis* Nutt., and *Onira* Ravenna are recognized in Cipurinae.

Rapid floral radiations accompanied by shifts between pollinator systems are well documented in Iridaceae (Goldblatt et al. 2002). Similar radiations with convergences and reversals may well be occurring within Tigridaeae in light of their remarkable variation in floral morphology and pollination syndromes (Rodriguez 1999). Additionally, flowers of *Tigridia* and related genera are strikingly similar to *Calochortus* (Liliaceae), an often co-occurring set of species that exhibits extensive parallelism in floral form, color, and pollination syndrome (Patterson and Givnish 2002, 2004). Such groups require careful evaluation of character conflict when analyzing data sets obtained from both morphology and molecules (Givnish and Sytsma 1997a, b; Givnish et al. 1999, 2005, 2006; Evans et al. 2000). Conditional combinability (Sytsma 1990; Bull et al. 1993; de Queiroz 1993; de Queiroz et al. 1995; Huelsenbeck et al. 1996; Johnson and Soltis 1998; Wiens 1998) is a conservative approach when studying such groups using both morphological and molecular characters.

As a first step in examining the phylogenetics, biogeography, and floral evolution within the tribe Tigridaeae, and

eventually the species-rich *Tigridia* (42 species) that exhibits a number of floral/pollination syndromes, we assess the phylogenetic relationships of Tigridaeae with both molecular and morphological characters. The objectives of this study are to: (1) infer phylogenetic relationships within the tribe Tigridaeae individually using morphological data, cpDNA, and ITS sequence data, (2) examine relationships based on combined evidence, and (3) use the phylogenetic framework obtained from these analyses to address the monophyly, biogeography, and origin of the subtribe Tigridiinae.

#### MATERIALS AND METHODS

##### Taxa and Plant Tissue

A total of 32 accessions including 23 taxa of Tigridaeae were analyzed for morphological, cpDNA sequence, and ITS sequence variation. Taxon sampling included all five genera of Tigridiinae and six of 13 genera of Cipurinae (Table 1). The genus *Rigidella* was included in *Tigridia* by Goldblatt (1990). Two genera (three species) of closely related tribe Mariceae (Reeves et al. 2001), and one genus each of tribe Sisyrinchieae and Irideae were also included. With this sampling, all four tribes of subfamily Iridoideae were represent-

ed (Goldblatt 1990). Leaf tissue was collected in the field for most taxa from Mexico (Rodriguez et al. 1996), dried and preserved in silica gel (Chase and Hillis 1991). Leaf tissue of *Calydorea pallens*, *Alophia veracruzana*, and one accession of *Nemastylis tenuis* were kindly provided by the San Antonio Botanical Gardens (San Antonio, Texas, USA), Yucca Do Nursery (Waller, Texas, USA), and Southwestern Native Seeds (Tucson, Arizona, USA), respectively. Finally, leaf material of *Tigridia lutea* was obtained from Peru and *Ennealophus foliosus* was collected in Ecuador. Voucher specimens (Table 1) are deposited at the Institute of Botany, University of Guadalajara Herbarium (IBUG) and the Wisconsin State Herbarium of the University of Wisconsin (WIS).

#### DNA Extraction

Total DNA was extracted using the method of Doyle and Doyle (1987, 1990) as modified in Smith et al. (1991). Extractions were performed on silica gel-dried leaf material from several individuals prepared in the field (Rodriguez et al. 1996). In some cases, fresh leaves were taken from plants grown at the Department of Botany of the University of Wisconsin greenhouse from bulbs collected in the field.

#### DNA Amplification, DNA Sequencing, and DNA Alignment

Primers for DNA amplification of the noncoding *trnT-trnL* and *trnL-trnF* cpDNA regions were as published by Taberlet et al. (1991). Likewise, the primer sequences used for the amplification of the *psbA-trnH* intergenic spacer are found in Sang et al. (1997). The reaction profile included an initial denaturation step at 94°C for 5 min, followed by 35 cycles with denaturation at 94°C for 30 sec, annealing at 48°C for 1 min and extension at 72°C for 1.5 min; a final elongation at 72°C for 7 min closed the amplification.

The nuclear ITS region, including ITS-1, ITS-2, the 5.8S rRNA gene, and flanking regions of the 18S and 26S genes, was amplified using the primers ITS5, ITSLeu.1, and ITS4 (White et al. 1990; Baldwin 1992). In some cases, the ITS region was amplified in two steps. In the first step, the ITS-1 was amplified using the primers ITS5 and ITS2. In the second step, the ITS-2 was amplified using the primers ITS3B and ITS4 (Baum et al. 1994). The primers ITS2, ITS4, and ITS5 are universal primers proposed by White et al. (1990). The reaction profile included an initial denaturation step at 94°C for 3 min, followed by 25 cycles with denaturation at 94°C for 1.5 min, annealing at 54°C for 2 min and extension at 72°C for 3 min; a last elongation at 72°C for 15 min closed the amplification.

Two methods were used to clean the PCR products. Ultrafree-MC Centrifugal Filter Units (Millipore Co., Billerica, Massachusetts, USA) were used following the manufacturer's specifications. Alternatively, PCR products were treated with the enzymes Exonuclease I, to degrade the primers and extraneous single stranded DNA, and Shrimp Alkaline Phosphatase (SAP: Amersham Life Sciences, Piscataway, New Jersey, USA), to remove unincorporated nucleotides.

Sequencing was performed using the ABI PRISM DNA Dye Terminator Cycle Sequencing Ready Reaction Kit or Big Dye 3.0 (Perkin-Elmer Applied Biosystems, Wellesley, Massachusetts, USA) following the protocols provided by

manufacturer. Subsequently, the sequences were visualized using the ABI 373 DNA Sequencer (Perkin-Elmer Applied Biosystems, Wellesley, Massachusetts, USA) at the DNA Synthesis and Sequencing Facility, University of Wisconsin Biotechnology Center. Sequence editing and alignment was carried out using the software program Sequencher 3.0 (Gene Codes Corporation, Ann Arbor, Michigan, USA). Improvement of the sequence alignment was done using the multiple alignment algorithms of CLUSTALX (Thompson et al. 1994, 1997) followed by manual refinement.

#### Morphological Data

The morphological data matrix was obtained from published literature and observations on more than 654 herbarium specimens deposited in the following herbaria: CHAPA, ENCB, F, IBUG, MEXU, MICH, MO, WIS, and ZEA. In addition, collecting expeditions were conducted in Mexico and Guatemala in 1995 and 1996 to collect and observe the species in their natural habitat (Rodriguez et al. 1996). The 40 qualitative characters used in the study consisted of 28 binary and 12 unordered multistate characters (Table 2). Thirty-eight characters were obtained from macromorphology, one from cytology, and one from palynology.

#### Phylogenetic Analyses

All phylogenetic analyses were conducted using maximum parsimony in using PAUP\* vers. 4.0b10 (Swofford 2002) on a Macintosh G4 using *Iris* as the ultimate outgroup (Reeves et al. 2001). Phylogenetic signal was estimated using the consistency index (CI), retention index (RI), rescaled consistency index (RC), and the permutation tail probability test (PTP). The PTP test was calculated from 10,000 Random Permutations of the original data. Shortest trees from each permuted matrix were searched with MulTree off, 10 Random Sequence additions and the Nearest Neighbor Interchange (NNI) branch-swapping algorithm. The Steepest Descent option was in effect. Heuristic approaches were used to find optimal trees. Searches were carried out using Fitch parsimony only on the potentially informative characters. Gap sites were incorporated into the analyses as missing characters. The heuristic searches were carried out with 1000 replicates of Random Sequence additions, MulTree off, and TBR branch-swapping.

Support for the different branches of the cladogram was assessed using the bootstrap (Felsenstein 1985) and decay (Bremer 1988) analyses. Bootstrap values were calculated with MulTree off and the TBR branch-swapping algorithm with 10 Random Sequence additions for each of the 1000 bootstrap replicates. The decay values were obtained by invoking the Enforce Topological Constraints option and keeping trees that were not compatible with the constraints as described in Baum et al. (1994). Heuristic searches included the activation of 100 Random Sequence additions, MulTree off, and TBR branch-swapping. The combined analysis of the morphology, cpDNA, and ITS data sets followed that of de Queiroz et al. (1995) and Wiens (1998).

#### Character and Taxonomic Congruence

The Mickevich-Farris ( $I_{MF}$ ; Mickevich and Farris 1981) and the Miyamoto ( $I_M$ ; Swofford 1991) incongruence indices

Table 2. Morphological characters and character states used in the cladistic analysis of Tigridaeae. All character states were scored as unordered. Polymorphic multistate characters were specified as polymorphic for the specific states found in that species.

Characters	Character states
1. Rootstock	0 = rhizome; 1 = bulb
2. Leaves	0 = ensiform; 1 = plicate; 2 = foliated
3. Basal leaves	0 = present; 1 = absent
4. Cauline leaves	0 = several; 1 = one
5. Flowering pattern	0 = leaves develop first; 1 = flower-producing stem develops first
6. Flowering stem	0 = winged; 1 = terete
7. Flowering stem branching	0 = branched; 1 = unbranched
8. Rhipidia	0 = pedunculate; 1 = sessile
9. Number of flowers per rhipidium	0 = several to few-flowered; 1 = single flowered
10. Blooming timing	0 = early-morning; 1 = mid-morning; 2 = early afternoon; 3 = late afternoon
11. Flower condition	0 = pedicellate; 1 = sessile
12. Flower position	0 = erect; 1 = secund; 2 = nodding
13. Flower shape	0 = flat; 1 = bowl; 2 = tubular
14. Flower color	0 = white; 1 = shades of yellow to orange; 2 = blue; 3 = red; 4 = dark
15. Flower odor	0 = none; 1 = sweetly fragrant; 2 = fetid
16. Pollination syndrome	0 = bees and wasps; 1 = butterflies; 2 = flies; 3 = hummingbirds
17. Tepal condition	0 = free; 1 = connate at base
18. Tepal shape	0 = not clawed; 1 = clearly divided into a limb and a claw
19. Inner tepal limb	0 = well developed; 1 = reduced
20. Nectaries	0 = lacking; 1 = present
21. Nectary location	0 = on outer tepals; 1 = on inner tepals
22. Nectary condition	0 = superficial and exposed; 1 = covered in a groove
23. Stamen-style branch apparatus	0 = scarcely or not exerted; 1 = well exerted
24. Filaments	0 = free; 1 = connate
25. Anther arrangement	0 = alternate to style branches; 1 = opposite to style branches
26. Anther position	0 = separated from style branches; 1 = adpressed to style branches
27. Anther orientation	0 = erect; 1 = diverge at an angle from staminal column
28. Anther dehiscence	0 = loculicidal; 1 = poricidal
29. Style position	0 = central; 1 = eccentric
30. Style shape	0 = lobed or divided above the anthers; 1 = deeply three-forked to the base of the anthers
31. Style branches	0 = filiform; 1 = thickened and cuneate; 2 = flattened and petaloid
32. Style branch shape	0 = undivided or apically lobed; 1 = deeply forked into two arms
33. Style arms	0 = erect; 1 = divaricate at an angle relative to staminal column
34. Style arm apex	0 = filiform; 1 = crested; 2 = cucullate
35. Stigmas	0 = terminal; 1 = transverse, at crests base
36. Arms mucro	0 = absent; 1 = present
37. Pollen grains	0 = monosulcate, spirate-sulcate, trichotomosulcate; 1 = zonosulcate; 2 = disulcate
38. Fruit shape	0 = clavate or oblong; 1 = subglobose; 2 = fusiform
39. Fruit dehiscence	0 = along the sides; 1 = by three apical valves
40. Gametophytic chromosome number	0 = $n$ = neither 7 nor 14; 1 = $n$ = 7; 2 = $n$ = 14

were calculated for all pairwise combinations of the morphological, ITS, and cpDNA data sets. The statistical significance of the  $I_{MF}$  and  $I_M$  values was determined using the incongruence length difference (ILD) test of Farris et al. (1995) as executed in PAUP\* using 1000 randomly selected partitions. The most-parsimonious trees were obtained with heuristic searches that included 10 Random Sequence additions with the options Steepest Descent, TBR branch-swapping, and MulTree off in effect.

For taxonomic congruence, a tree of trees analysis was performed following the method of Graham et al. (1998). This procedure generates a phenogram that graphically illustrates the similarity of all most-parsimonious trees obtained independently from different data sets, including trees from the combined data set. Trees that are significantly dif-

ferent in topology from trees generated from other data sets will be placed in remote portions of the "tree of trees."

## RESULTS

### Matrix Characteristics—Plastid Regions

The length of the *pbsA-trnH* spacer of Tigridaeae varied from 448 to 483 bp. The alignment for all 32 taxa required the insertion of 11 gaps 1–3 bp long. *Tigridia durangense*, *Trimezia fosteriana*, and *Trimezia martinicensis* shared a six-bp insertion. The aligned sequence length of the *pbsA-trnH* spacer was 495 bp.

Only the 5'-end of the *trnT-trnL* spacer was sequenced. The length of the *trnT-trnL* spacer varied in Tigridaeae from 330 in *Tigridia durangense* and *Rigidella inusitata* to 372 in

Table 3. Comparison of data variation and character-state reconstruction on most-parsimonious trees from separate and combined analyses of morphology, ITS, and cpDNA sequence data sets. M = Morphology, ITS = ITS sequence data, cpDNA = cpDNA sequence data, and C = combined data sets. The  $I_{MF}$  and  $I_M$  indices values between pairwise data sets are, respectively: M-ITS (0.09, 0.37); M-cpDNA (0.17, 0.43); ITS-cpDNA (0.05, 0.16).

	M	ITS	cpDNA	C
No. of potentially informative characters	36	231	127	394
No. of most-parsimonious trees	20	33	34	44
CI	0.46	0.59	0.55	0.53
RI	0.74	0.68	0.75	0.67
RC	0.34	0.40	0.41	0.36
Minimum tree length in absence of homoplasy	51	383	159	594
Observed tree length	111	648	287	1107
Number of extra steps	60	265	128	513
Tree length measured with morphological data	111	166–175	163–167	133–144
Tree length measured with ITS data	781–836	648	687–694	661–666
Tree length measured with cpDNA data	378–415	322–336	287	301–308
Tree lengths measured with combined data	1271–1357	1141–1160	1140–1148	1107

*Alophia veracruzana* and *Calydorea pallens*. *Trimezia martinicensis* was unique by having two deletions of 24 and 284 bp; the sequence length for this species was 135 bp. Because of ambiguities in the alignment, a 310-bp segment in *Iris versicolor* and *Sisyrinchium scabrum* was not included in the analysis. Several gaps were necessary to align the 32 accessions that produced a 443 bp final length alignment.

Within the tribe Tigridieae, sequence length of the *trnL-trnF* spacer ranged from 364 in *Cobana guatemalensis*, *Tigridia durangense*, and *Rigidella flammea* to 374 in *Cipura campanulata*. Sequences of the members of the tribe Mariceae varied from 364 in *Trimezia martinicensis* to 373 in *Trimezia fosteriana*. Several gaps were necessary to align the 32 accessions that yielded a final aligned sequence of 445 bp.

When all three noncoding regions were combined, 332 of the 1383 sites (24%) were variable. Of these sites, 127 are phylogenetically informative (Table 3); 37 occurred in *psbA-trnH* (29.13%), 44 in *trnT-trnL* (34.64%), and 46 in *trnL-trnF* (36.22%). When the number of phylogenetically informative sites was taken as a percentage of the number of variable positions for each of the three regions, the following values were seen: 48.05% (37/77) for *psbA-trnH*, 31.65% (44/139) for *trnT-trnL*, and 39.65% (46/116) for *trnL-trnF*.

#### Matrix Characteristics—Nuclear Regions

The boundaries of the ITS-1, 5.8 rDNA, and ITS-2 were determined by inspection and comparison with the published sequences from *Oryza sativa* L. (Takaiwa et al. 1985). ITS-1 ranged from 233 to 259 base pairs (bp). For most Tigridieae the 5.8S rDNAs were 163–167 bp in length. ITS-2 varied from 208 to 264. The alignment of the ITS sequences for all taxa required the introduction of several 1- to 6-bp gaps scattered in ITS-1 and ITS-2 regions. Two larger gaps of 26 and 20 bp in ITS-2 were required. Finally, the aligned sequence length of the ITS region, including ITS-1, ITS-2, the 5.8S rRNA gene, and flanking regions of the 18S and 26S genes was 773 bp. ITS exhibited 231 potentially informative characters (Table 3).

#### Phylogenetic Results

The phylogenetic analysis of morphological characters generated 20 most-parsimonious trees of 111 steps, CI = 0.46, RI = 0.74, and RC = 0.34 (Table 3). One of these trees is illustrated in Fig. 1 to show branch lengths and support values. Considering the suspected plasticity of floral characters in the tribe Tigridieae and the low number of cladistically informative characters (36) relative to molecular characters, it is not surprising that the resulting cladograms showed weakly supported branches and that the strict consensus tree resolved only eight branches (see Fig. 1).

The cpDNA data set was found to possess significant cladistic signal based on the PTP ( $P < 0.001$ ) and the cladistic analysis yielded 34 trees of 287 steps, CI = 0.55, RI = 0.75, and RC = 0.41 (Table 3). One of the most-parsimonious trees is illustrated in Fig. 2. The strict consensus identified two major clades without statistical support and failed to sustain the monophyly of the tribe Tigridieae (see Fig. 2). The first clade was poorly supported and showed a sister group relationship between most members of subtribe Cipurinae (Tigridieae) and tribe Mariceae represented by *Trimezia martinicensis*, *Trimezia fosteriana*, and *Neomarica gracilis*. Sister to this clade is a group, hereafter referred to as the Tigridiinae clade, which could be further separated into the Mexican-Guatemalan Tigridiinae and an assemblage of Tigridiinae-Cipurinae taxa including *Alophia veracruzana*, *Tigridia lutea*, *Ennealophus foliosus*, and *Eleutherine latifolia*. The Mexican-Guatemalan Tigridiinae were well supported as a monophyletic group and included two taxa, *Cardiostigma longispatha* and *Nemastylis convoluta*, previously recognized as members of Cipurinae. Cladistic analyses with and without *Tigridia lutea* generated trees with similar topologies. The *trnT-trnL* spacer was not sequenced for this species despite considerable effort and time allocation.

The phylogenetic analysis of the ITS sequence data yielded 33 most-parsimonious trees of 648 steps, CI = 0.59, RI = 0.68, and RC = 0.40 (Table 3). One of the most-parsimonious trees is illustrated in Fig. 3 to show branch lengths and support values. In contrast to cpDNA data, the ITS strict consensus tree (see Fig. 3) supported a monophyletic tribe

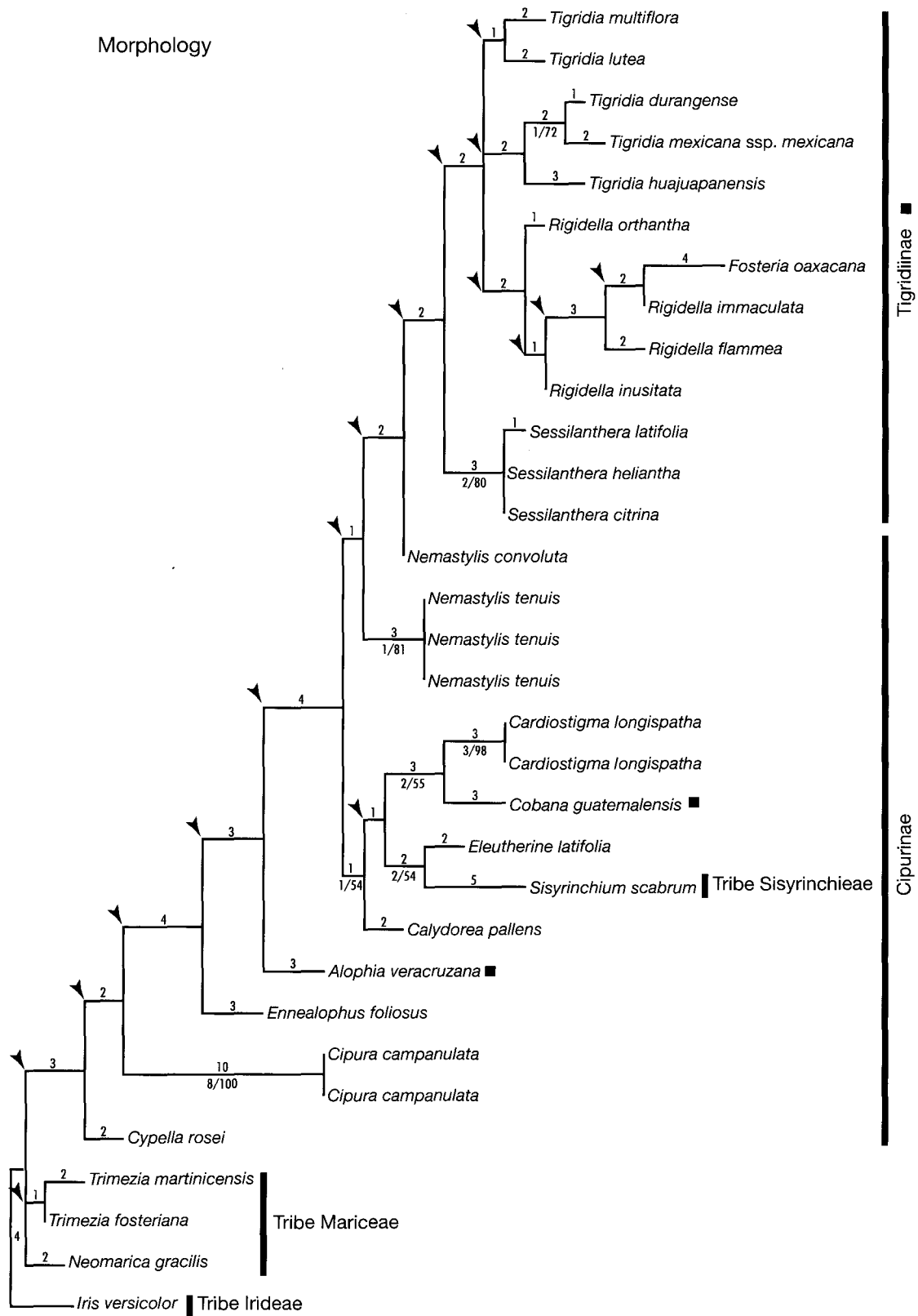


Fig. 1.—One of 20 most-parsimonious trees obtained from the cladistic analysis of morphological variation. Tree length = 111, CI = 0.46, RI = 0.74, RC = 0.34. Numbers above branches represent branch length. Decay indices/bootstrap values (>50%) are given below the branch. Arrows indicate branches that collapse in the strict consensus tree.

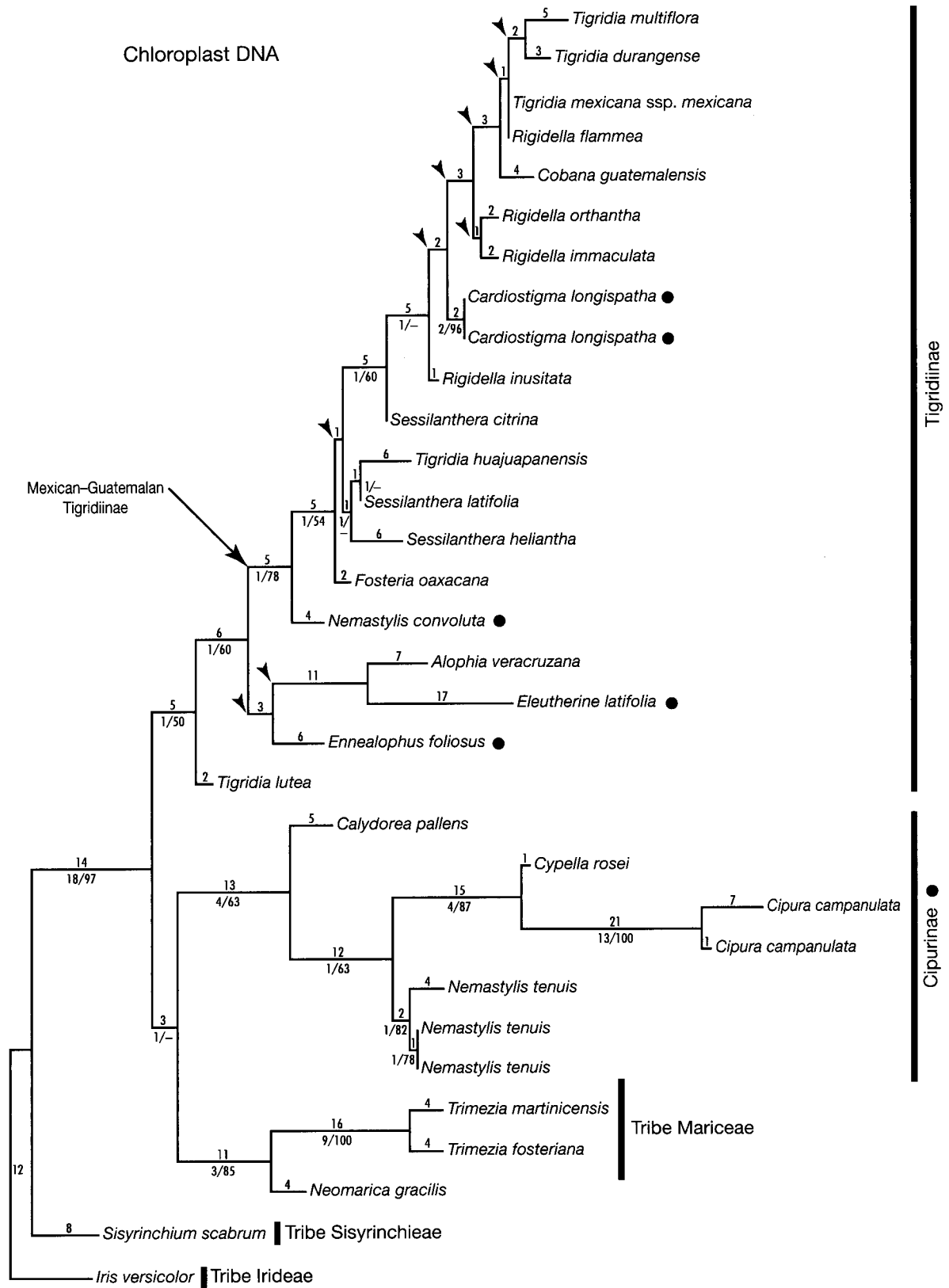


Fig. 2.—One of 34 most-parsimonious trees obtained from the cladistic analysis of three cpDNA spacers sequence variation. Tree length = 287, CI = 0.55, RI = 0.75, RC = 0.41. Numbers above branches represent branch length. Decay indices/bootstrap values (>50%) are given below the branch. Arrows indicate branches that collapse in the strict consensus tree.



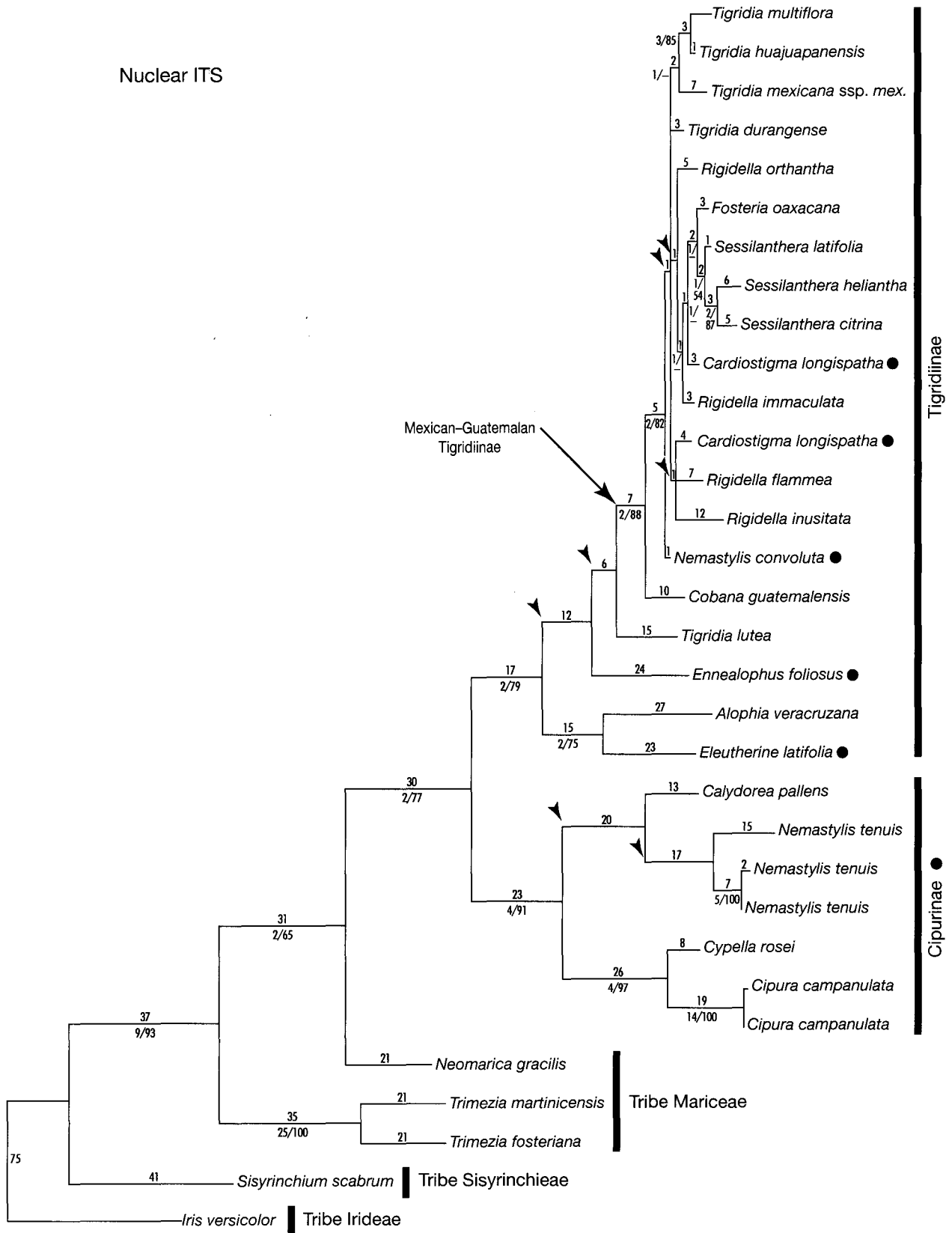


Fig. 3.—One of 33 most-parsimonious trees obtained from the cladistic analysis of ITS sequence variation. Tree length = 648, CI = 0.59, RI = 0.68, RC = 0.40. Numbers above branches represent branch length. Decay indices/bootstrap values (>50%) are given below the branch. Arrows indicate branches that collapse in the strict consensus tree.

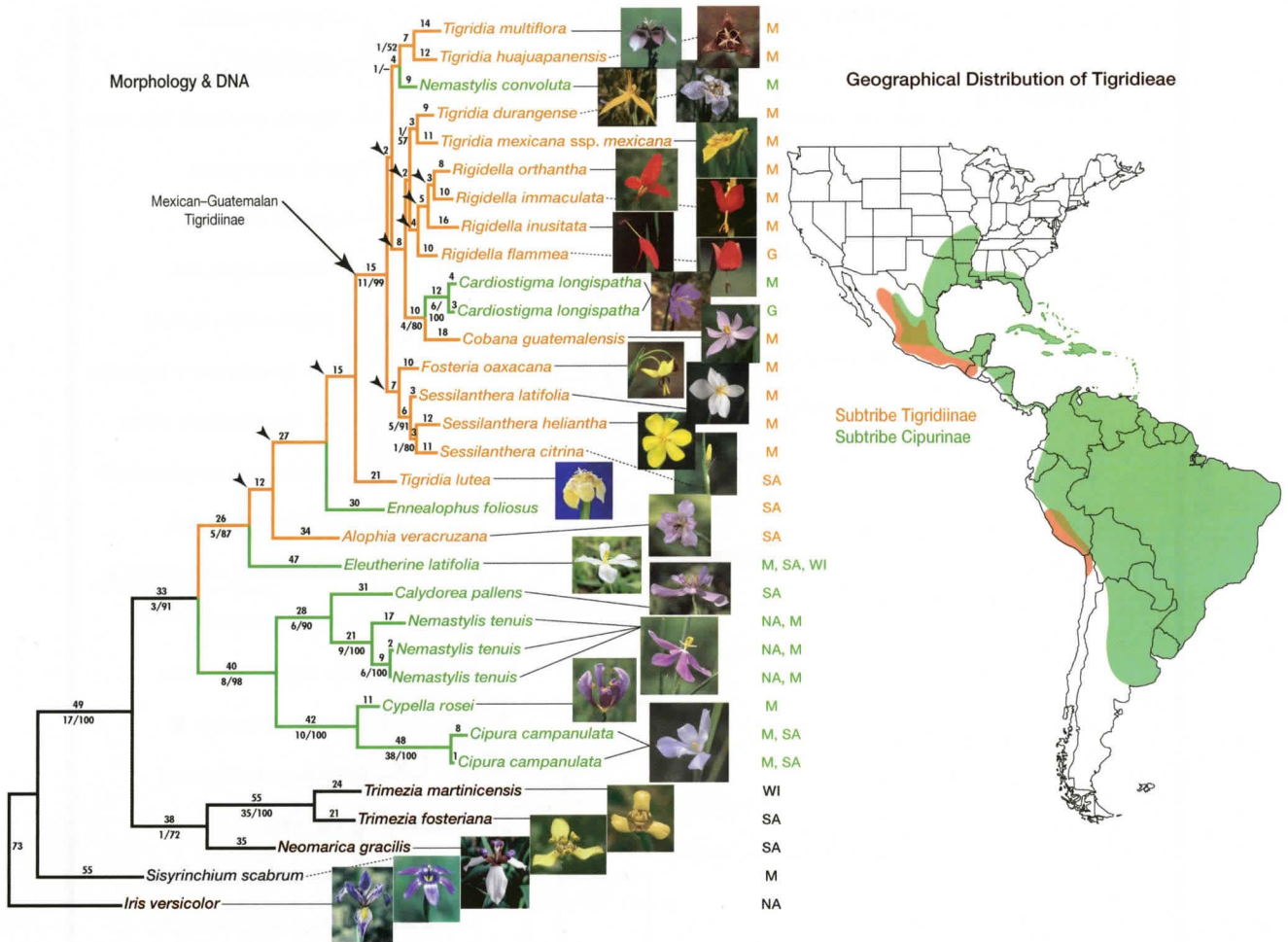


Fig. 4.—One of 44 most-parsimonious trees obtained from the cladistic analysis of morphological variation, cpDNA sequence, and ITS sequence variation. Tree length = 1107, CI = 0.53, RI = 0.67, RC = 0.36. Numbers above branches represent branch length. Decay indices/bootstrap values (>50%) are given below the branch. Arrows indicate branches that collapse in the strict consensus tree. Floral images of each species are provided to the right. Species placement in the two subtribes of Tigridieae is indicated by color. Geographical location of each species is indicated by M (Mexico), G (Guatemala), WI (West Indies), SA (South America), or NA (North America). Geographical distributions of the two subtribes are shown in color.

Tigridieae with two well-supported clades. The first clade comprised only genera of the subtribe Cipurinae (*Calydorea*, *Cipura*, *Cypella*, and *Nemastylis*) and the second corresponded to the subtribe Tigridiinae plus *Eleutherine*, *Ennealophus*, *Cardiostigma* Baker, and *Nemastylis convoluta*, the latter previously recognized as genera of the subtribe Cipurinae. Additionally, the Tigridiinae clade included a strongly supported monophyletic Mexican-Guatemalan Tigridiinae and an unresolved basal group formed by *Tigridia lutea*, *Alophia veracruzana*, *Ennealophus foliosus*, and *Eleutherine latifolia*.

The combined morphological, ITS sequence, and cpDNA sequence data set resulted in 2196 characters; 394 were parsimony informative, including 36 morphological characters, 231 ITS nucleotide positions, and 127 cpDNA nucleotide changes. Cladistic analysis of the entire data set resulted in 44 most-parsimonious trees with 1107 steps, CI = 0.53, RI = 0.67, and RC = 0.36 (Table 3). One of these trees is illustrated in Fig. 4 and shows branches collapsing in the strict consensus tree. The strict consensus tree strongly supports a monophyletic tribe Tigridieae with two main clades.

The first clade comprises some of the traditionally recognized members of Cipurinae: *Calydorea*, *Nemastylis*, *Cipura*, and *Cypella*. The second clade includes all members of the subtribe Tigridiinae and the remaining genera of the subtribe Cipurinae included in this study (*Eleutherine*, *Ennealophus*, *Cardiostigma*, and *Nemastylis convoluta*). Additionally, the Tigridiinae clade contains a monophyletic Mexican-Guatemalan Tigridiinae and a basal polytomy comprising *Tigridia lutea*, *Alophia veracruzana*, *Ennealophus foliosus*, and *Eleutherine latifolia*. The monophyletic Mexican-Guatemalan Tigridiinae also includes two taxa usually placed in Cipurinae: *Cardiostigma longispatha* and *Nemastylis convoluta*. The total evidence tree identifies the subtribe Cipurinae, as currently defined, as a paraphyletic lineage.

#### Character Congruence

The  $I_{MF}$  computes the incongruence between data sets as the number of extra steps needed by each individual data set to explain the most-parsimonious trees retrieved from analysis of the combined data. Likewise, the  $I_M$  estimates char-

acter incongruence by summing the number of extra steps required to map data set X on the shortest trees recovered from data set Y with the number of extra steps required to map data set Y on the shortest trees recovered from data X. The  $I_M$  values were calculated using the trees requiring the fewest additional steps. Table 3 describes and compares the phylogenetic results of the morphological, ITS sequence, cpDNA sequence, and combined data sets. The  $I_{MF}$  values indicate varying levels of incongruence from a low of 5% between the two molecular data sets to a high of 17% between morphology and cpDNA. In contrast, the  $I_M$  values show between three and four times as much between-data-set incongruence as does  $I_{MF}$ , but again with the lowest values between the two molecular data sets. When data sets were tested for incongruence using the ILD test, the deviation from the expected values was found to be significant. The results of ILD test applied to three pairs of data partitions and the three data sets combined are as follows: morphology–cpDNA ( $P = 0.01$ ), morphology–ITS ( $P = 0.01$ ), cpDNA–ITS ( $P = 0.03$ ), and cpDNA–morphology–ITS ( $P = 0.001$ ).

#### Taxonomic Congruence

The cladistic analyses of the independent data sets produced 20, 33, and 34 most-parsimonious trees from morphological, ITS, and cpDNA variation, respectively. All pairwise data combinations among the data sets yielded 3, 27, and 2 trees from morphology–ITS, morphology–cpDNA, and ITS–cpDNA, respectively. Lastly, analysis of all data combined (morphology–ITS–cpDNA) produced 44 most-parsimonious trees. The total of 163 trees resulting from all analyses were graphically compared using the tree of trees method (Graham et al. 1998). The resulting phenogram (not shown) indicated that the cladograms derived from morphology to be the most topologically distinct within the set of all trees examined (morphology, ITS, cpDNA, and various combined data) and to be the set with most divergent trees.

### DISCUSSION

#### Phylogenetic Congruence

Based on a rigid adherence to the ILD test (and to a lesser extent on  $I_M$  and  $I_{MF}$  values), the null hypothesis of congruence would be almost certainly invalid and data sets should not be combined. The ILD test found the morphological data set to be statistically different from the cpDNA and ITS data sets ( $P = 0.01$ ). Similarly, the  $P$  value estimated for the three data sets together was 0.001. In contrast, The ILD test was only slightly significant ( $P = 0.03$ ) between the cpDNA and the ITS data. The ILD test (and similar tests of congruence), however, should best be viewed as a first estimate in examination of congruence or the lack thereof between different data sets (Cunningham 1997; Yoder et al. 2001; Hipp et al. 2004). We argue that further analysis of these data sets supports conditional combination of the three data sets as specific factors generating much of the incongruence can be identified. The conflict between analyses appears to be due to both a lack of phylogenetic signal in the separate data sets (sometimes in different regions of the tree) and the displace-

ment of two taxa (*Tigridia huaquapanensis* and *Cobana guatemalensis*) from moderately supported branches in the nuclear vs. chloroplast DNA trees (Fig. 2, 3). These two species are placed in the combined data set tree (Fig. 4) in positions identified by ITS and cpDNA, respectively. Further analyses are underway to determine the exact nature of these two discrepancies.

The phylogenetic analysis of morphological data does not support a monophyletic tribe Tigridaeae as there is no resolution at the base of the tree (Fig. 1). Many branches in the cladogram are not well supported and the strict consensus tree resolves only eight clades (Fig. 1). The lack of branch support in the morphology trees is due to both few potentially informative characters (36) and fairly high levels of homoplasy (54%). In contrast, the cladograms obtained in both cpDNA and ITS analyses show support for many more branches and phylogenetic insight within the tribe Tigridaeae can be obtained from them (Fig. 2, 3). The results of the two molecular analyses are congruent with respect to certain major features of Tigridaeae phylogeny. Most important, they support the recognition of two main clades; the first comprising only members of subtribe Cipurinae and the second comprising all members of subtribe Tigridiinae and some Cipurinae. The two molecular based trees are in conflict with respect to the monophyly of the tribe Tigridaeae and the branching order within the subtribe Tigridiinae. These conflicts, however, reside in regions of the trees where relatively few characters are available for either the cpDNA or ITS data sets. For example, cpDNA does not identify a monophyletic tribe Tigridaeae, as the subtribe Cipurinae is sister (although with little support) to the tribe Mariceae (Fig. 2). Similarly, ITS does not identify a monophyletic tribe Mariceae, as *Neomarica* is placed as sister to the tribe Tigridaeae (Fig. 3).

The analysis of all three data sets combined provides the best supported estimate of phylogeny for the tribe Tigridaeae based on bootstrap and decay values (Fig. 4). The general result of the bootstrap analysis is that the three data sets tended to reinforce each other in cases where they are congruent. The tribe Tigridaeae (91%), the subtribe Tigridiinae (99%), and the subtribe Cipurinae (98%) formed clades at bootstrap values with higher frequencies than those in the separate analyses (Fig. 4). The Mexican-Guatemalan Tigridiinae, *Tigridia lutea*, *Alophia veracruzana*, *Eleutherine latifolia*, and *Ennealophus foliosus* were united at the 87% level, rather than at 20% as in the morphological analysis, 50% as in the cpDNA, and 79% as in the ITS alone. The cladograms obtained from the combined molecular data (cpDNA + ITS; not shown) and total evidence show nearly identical relationships except for weakly-supported branches.

#### Classification—Issue of Floral Convergence

The results presented in this study show only partial concordance with the current classification of the tribe Tigridaeae (Goldblatt 1990). The total evidence cladogram supports the tribe Tigridaeae as a monophyletic group and its sister relationship to the tribe Mariceae, but disagrees with the circumscription of the subtribes Cipurinae and Tigridiinae (Fig. 4). *Tigridia* is also clearly not monophyletic in

any of the molecular or combined data cladograms (Fig. 2–4), although the five species sampled form a clade with morphology (Fig. 1). A broader survey of *Tigridia* supports the non-monophyly of the genus (Rodriguez 1999).

This discrepancy in relationships, as seen with morphology vs. molecules, suggests that parallelism in floral features may be an important evolutionary phenomenon in Tigridieae as it has been documented in co-occurring *Calochortus* (Patterson and Givnish 2002, 2004). A comparison of levels of homoplasy of certain morphological characters illustrates this phenomenon (see Evans et al. 2000 for similar study). Only two characters, rootstock (1) and pollen grains (37) are less homoplasious in the molecular trees relative to the morphological tree. Notably, the bulbous rootstock is one of the nonfloral characters that define the tribe Tigridieae. Conversely, pollination syndromes (16) and related characters such as tepal shape (18), presence of nectaries (20), nectary condition (22), anther arrangement (25), style branches (31), style arm apices (34), and stigmas (35) showed considerably greater levels of homoplasy in the molecular trees relative to the morphological tree. Importantly, the cladistic analysis of morphological data tends to associate taxa with similar pollination syndromes whereas molecular data suggest that such groupings might include phylogenetically unrelated taxa.

#### Biogeographical Implications

Based on total evidence, the phylogenetic reconstruction of the tribe Tigridieae suggests a South American origin of the monophyletic Mexican-Guatemalan Tigridiinae (Fig. 4). This hypothesis is corroborated by the correlation between the geographical distribution of *Tigridia lutea*, *Ennealophus foliosus*, *Alophia veracruzana*, and *Eleutherine latifolia* and their placement as either a basal grade or unresolved polytomy with respect to the Mexican-Guatemalan Tigridiinae based on total evidence. *Ennealophus* is a South American genus of five species. Specifically, *Ennealophus foliosus* grows in Peru, Brazil, and Bolivia (Ravenna 1977). *Tigridia lutea* is found only in the coastal lomas of Peru (Ravenna 1976). *Alophia*, a genus of four species, ranges from the southern United States through the Mexican Atlantic slope to Brazil. *Alophia veracruzana* is endemic to Veracruz, Mexico (Goldblatt and Howard 1992). Correspondingly, the genus *Eleutherine* comprises two species that range from eastern Mexico through the West Indies to Bolivia and southeastern Brazil. Thus, the current geographical distribution of these taxa and their positions on the cladogram obtained from the total evidence suggest a northward migration from South America with a final radiation in Mexico.

The geographical distribution of *Cipura campanulata*, *Cypella rosei*, *Nemastylis tenuis*, and *Calydorea pallens* and their positions in the total phylogenetic evidence require further explanation. *Cipura campanulata*, *Cypella rosei*, and *Nemastylis tenuis* grow sympatrically with some species of *Tigridia* in Mexico. Yet, the phylogenetic results show these taxa to be more distantly related to subtribe Tigridiinae than *Tigridia lutea*, *Ennealophus foliosus*, *Alophia veracruzana*, and *Eleutherine latifolia*. *Nemastylis* is a genus of five species found in the United States and Mexico, with *Nemastylis tenuis* representing its southern-most limit. *Cipura* is a genus

of six species distributed from western Mexico through Central America and the West Indies to Brazil and Bolivia. Specifically, *Cipura campanulata* extends from western Mexico through Central America to northern Venezuela and Colombia. *Cypella rosei* represents one of only two Mexican species of this South American genus. Lastly, *Calydorea* is a South American genus with *Calydorea pallens* restricted to South Central Argentina. Based on this geographical scenario, a hypothesis might have involved several migration waves of Cipurinae species from South to North America. Tigridiinae could have originated from a South American lineage of which *Tigridia lutea*, *Ennealophus foliosus*, *Alophia veracruzana*, and *Eleutherine latifolia* would be extant representatives.

#### Conclusion

The results of these various phylogenetic analyses illustrate the utility of combining molecular and morphological data sets as well as analyzing them separately when appropriate. This procedure has the potential of resolving conflicts between data sets, particularly when character support is low for certain branches, suggesting that the lack of complete congruence among trees in this example reflects the absence of sufficient signal rather than fundamentally different evolutionary histories or unwieldy levels of convergence. In other cases, comparing the levels of homoplasy of specific morphological characters when applied to morphological or molecular cladograms demonstrates the phenomenon of floral parallelism. The more robust portions of the cladogram from the combined analysis, though clearly in need of support from future studies sampling more taxa and more character systems (both morphological and molecular), can serve as a framework for evolutionary and biogeographical interpretations. For example, the monophyly of Tigridieae is reasonably supported. The common origin of the North American Tigridiinae from a South American lineage is also clearly defined. The resulting phylogenies also suggest multiple migration waves of Tigridieae from South to North America. Lastly, and most importantly, the phylogenetic approach to this evolutionarily interesting group of plants has opened new avenues for future research and the raising of new questions previously not articulated.

#### ACKNOWLEDGMENTS

We thank Kandis Elliot for her support on artwork. Thanks, as always, are extended to those in charge of herbaria for loans (CHAPA, ENCB, F, IBUG, MEXU, MICH, MO, WIS, and ZEA). This work was supported by a scholarship to Aaron Rodriguez from the University of Guadalajara (Expediente BC/1925/94). Collecting expeditions and laboratory work were supported in part by the Comisión Nacional para el Conocimiento y Uso de la Biodiversidad, México (CONABIO: Convenio No. FB355/J089/96), the Davis Fund of the Department of Botany, University of Wisconsin, the University of Wisconsin Natural History Museums Council, and the American Iris Society.

#### LITERATURE CITED

- BALDWIN, B. G. 1992. Phylogenetic utility of the internal transcribed spacers of nuclear ribosomal DNA in plants: an example from the Compositae. *Molec. Phylogen. Evol.* 1: 3–16.



- Miyamoto and J. Cracraft [eds.], Phylogenetic analysis of DNA sequences. Oxford University Press, Oxford, UK.
- . 2002. PAUP\*: phylogenetic analysis using parsimony (\*and other methods), vers. 4.0. Sinauer Associates, Inc., Sunderland, Massachusetts, USA.
- SYTSMA, K. J. 1990. DNA and morphology: inference of plant phylogeny. *Trends Ecol. Evol.* **5**: 104–110.
- TABERLET, P., L. GIELLY, G. PAUTOU, AND J. BOUVET. 1991. Universal primers for amplification of three non-coding regions of chloroplast DNA. *Pl. Molec. Biol.* **17**: 1105–1109.
- TAKAIWA, F., K. OONO, AND M. SIGIURA. 1985. Nucleotide sequence of the 17S–25S spacer region from rice rDNA. *Pl. Molec. Biol.* **4**: 355–364.
- THOMPSON, J. D., T. J. GIBSON, F. PLEWNIAC, F. JEANMOUGIN, AND D. G. HIGGINS. 1997. The CLUSTAL\_X windows interface: flexible strategies for multiple sequence alignment aided by quality analysis tools. *Nucl. Acids Res.* **25**: 4876–4882.
- , D. G. HIGGINS, AND T. J. GIBSON. 1994. CLUSTAL W: improving the sensitivity of progressive multiple sequence alignment through sequence weighting, position-specific gap penalties and weight matrix choice. *Nucl. Acids Res.* **22**: 4673–4680.
- WHITE, T. J., T. BRUNS, S. LEE, AND J. TAYLOR. 1990. Amplification and direct sequencing of fungal ribosomal RNA genes for phylogenetics, pp. 315–322. In M. Innis, D. Gelfand, J. Sninsky, and T. White [eds.], PCR protocols: a guide to methods and applications. Academic Press, San Diego, California, USA.
- WIENS, J. J. 1998. Combining data sets with different phylogenetic histories. *Syst. Biol.* **47**: 568–581.
- YODER, A. D., J. A. IRWIN, AND B. A. PAYSEUR. 2001. Failure of the ILD to determine data combinability for slow loris phylogeny. *Syst. Biol.* **50**: 408–424.